

Deterministic versus reliability-based topology optimization of aeronautical structures

Carlos López¹ · Aitor Baldomir¹ · Santiago Hernández¹

Received: 28 January 2015 / Revised: 17 September 2015 / Accepted: 2 November 2015 / Published online: 20 November 2015
© Springer-Verlag Berlin Heidelberg 2015

Abstract Aircraft design is a challenging process which is constantly looking for developing new and lighter structural components. The application of topology optimization techniques is growing widespread in the aeronautical industry as it has proven to be highly useful for saving important weight amounts in recent aircraft designs. The objective of this research is to obtain optimal and novel aeronautical architectures through topology optimization while considering uncertainty in loads and material properties. For this, a methodology that combines the Sequential Optimization and Reliability Assessment (SORA) with external optimization software has been developed in order to perform Reliability-Based Topology Optimization (RBTO). The methodology is then compared against the classical way of obtaining novel architectures in aeronautical industry, which lie in the application of Deterministic Topology Optimization (DTO) considering partial safety factors in some data influencing the structural responses. The comparison draws weight savings of up to 3 % in the examples proposed when applying RBTO which could be highly significant in an aircraft structure. Moreover it has been proven that when performing a RBTO approach the layout of the final design can be different depending on the safety level required, which may influence the next phases of aircraft design process.

Keywords Uncertainty · Topology optimization · Reliability · Aircraft design

✉ Carlos López
carlos.lopez.rodriguez@udc.es

¹ Structural Mechanics Research Group, School of Civil Engineering, Universidade da Coruña, Campus de Elviña s/n, 15071 A Coruña, Spain

1 Introduction

Aeronautical industry is always seeking for new and novel aircraft architectures as well as redesigning classical components so as to address the next generation of aircrafts, which tend to be lighter, cleaner and safer, making the application of Deterministic Topology Optimization (DTO) techniques a useful tool for reaching that target. This discipline has been used for the last decade by most of the main aircraft companies, as Airbus (Grihon et al. 2004; Krog et al. 2004; Krog and Tucker 2002), Bombardier (Buchanan 2007), Boeing (Wang et al. 2011) or Embraer (Santos Iwamura and Rocha de Faria A 2013), as well as by many researchers (Maute and Allen 2004; Maute and Reich 2006; Stanford and Ifju 2009; Stanford et al. 2012; Stanford and Dunning 2014 or James et al. 2014) due to its capacity to generate unconventional structural architectures which are usually lighter than classical ones. In aeronautical industry this new structural schemes are generally later converted into manufactural structures through a concept design definition and then re-tuned by applying size and shape optimization techniques.

Topology optimization was used in the design of Airbus A380, the largest commercial aircraft in the world, leading to an overall weight savings of 1000 kg per aircraft. This was mainly thanks to the redesign of the inboard inner and outer fixed leading edge ribs and the fuselage door intercostals (Grihon et al. 2004). Moreover, in Krog et al. (2004) new wing box rib architectures were obtained through topology optimization using global and local approaches combining several different formulations. These include the classical minimum global compliance formulation and a mini-max global compliance formulation, both with a volume fraction constraint, as well as an alternative minimum weight with constrained compliance formulation. More recently, Bombardier has also employed topology optimization in the novel design of two-

dimensional wing box ribs applying a minimum global compliance with volume fraction constraint formulation. Then they define the structural concept design from the topology layout, which is finally re-tuned using size and shape optimization so as to provide a manufactural aircraft component (Buchanan 2007). Boeing also applied this discipline to the preliminary design of the wing leading-edge structure of the 787 Dreamliner, reaching to a 25–45 % lighter design compared with the wing of the Boeing 777 (Wang et al. 2011).

Furthermore, aircraft design is a challenging process that links several multidisciplinary areas and needs to take into account several uncertain data to address the best possible design, while accomplishing the restrictive safety targets imposed by international regulations. This leads to the imposition of safety factors during the whole design process that sometimes are based on experience and lack of scientific basis, being a key aspect to be further studied. Uncertain data in loads, material properties, manufacture processes, etc. need to be included as random variables in the different aircraft design phases, particularly during the preliminary stage where DTO is employed.

Reliability-Based Topology Optimization (RBTO) combines statistical and probabilistic design methods with topology optimization, and is being used by several authors of different research fields (Kang et al. 2004; Kim et al. 2007; Kang and Luo 2009 or Dunning et al. 2011). This discipline requires high computationally effort and may be unstable in terms of convergence depending on the problem. RBTO techniques are based on Reliability-Based Design Optimization (RBDO) methods, which are currently applied to industrial size and shape optimization problems (Youn et al. 2004; Zou and Mahadevan 2005; Kaushik 2007; Karadeniz et al. 2009 or Hernandez et al. 2013). However RBTO has not yet been applied in large three-dimensional models and thus it has not been proven to work for real like aero-structures.

In this paper the Sequential Optimization and Reliability Assessment (SORA) algorithm is implemented in an in-house computational code that calls external optimization software so as to perform complex industrial-like RBTO problems. The SORA is one of the most efficient RBDO single-loop methods as it offers robustness, suitability to complex structural systems and low computational effort compared against other methods (Aoues and Chateaneuf 2010). The methodology developed consists of combining the aforementioned in-house computational code, which manages the whole process and performs the reliability analysis, with commercial optimization software. This is later applied to real-like aeronautical structures involving a large number of design variables and degrees of freedom.

Topology of preliminary baseline models is crucial for the upcoming design phases. Depending on the safety level required by the engineers, the RBTO process will provide

different structural layouts that would condition the next phases of the aircraft design. Besides, RBTO based aircraft designs may lead to lighter structures than those provided by DTO as consequence of using the real distribution functions of random variables instead of partial safety factors in the design process. In this research we carry out a study between both approaches to determine which is the most efficient in terms of weight savings establishing a coherent comparison of results.

2 Reliability-based topology optimization applying the sequential optimization and reliability assessment

The general formulation of a RBTO problem can be expressed mathematically as follows:

$$\min F(\mathbf{d}_k) \quad (1.a)$$

subject to:

$$g_j(\mathbf{d}_k, \mathbf{x}_k) \leq 0 \quad (j = 1, \dots, m) \quad (1.b)$$

$$P[G_i(\mathbf{d}_k, \mathbf{x}_k) \leq 0] \leq P_{f,i} \quad (i = 1, \dots, n) \quad (1.c)$$

where \mathbf{d}_k and \mathbf{x}_k are the deterministic design and random variables for the k -esime optimization cycle, g_j is the j -esime deterministic constraint, G_i is the i -esime limit-state function, P is the probability operator and denotes the probability that has the limit-state function to be in a failure region, $P_{f,i}$ is the required probability of failure and m and n are the number of deterministic and probabilistic constraints, respectively.

The main difference between RBTO and the traditional DTO is that the uncertainty of some variables that influence the structural responses is included as random variables in the optimization process. First pieces of researches in this discipline employed the Reliability Index Approach (RIA) by Enevoldsen and Sorensen (1994) or Performance Measure Approach (PMA) by Tu et al. (1999) for solving RBTO problems in a variety of scientific disciplines (Jung and Cho 2004; Maute and Frangopol 2003 or Kim et al. 2006). Both algorithms belong to the so-called double-loop methods as they require an inner optimization loop to determine the probability of failure for each structural configuration and an outer loop that is the proper optimization problem. On the other hand, Kharmanda et al. (2004) developed a sequential procedure with three successive steps: sensitivity analysis, reliability index evaluation and deterministic topology optimization based on the traditional minimum compliance formulation with volume fraction constraint. More recently, Silva et al. (2010) developed a single-loop methodology able to consider either the failure of different events in a component RBTO or the embracement of all failure events in a system RBTO, while Nguyen et al. (2011) proposed a single-loop technique that considers the statistical dependence between several limit-states.

The methodology proposed is based on the RBDO algorithm Sequential Optimization and Reliability Assessment (SORA) developed by Du and Chen (2004) as it belongs to the so-called decoupled methods. This means that the algorithm separates the optimization problem from the reliability process avoiding nested loops, making it highly combinable with external optimization software and being suitable to perform complex structural systems. Moreover, according to Aoues and Chateaneuf (2010) the SORA has proven to be robust and accurate. The methodology developed allows taking profit from the capabilities of both the SORA and the external software, including robustness, accuracy and the consideration of uncertainty from the former as well as efficiency, accuracy and low computational effort in solving large optimization problems from the latter. Other well-known RBDO algorithms, like RIA or PMA, would not be adequate because the combination of external optimization software within them would be troublesome from the point of view of computational effort.

The aforementioned methodology consists of solving a sequence of deterministic topology optimizations, each followed by a reliability analysis that evaluates the probability of failure of the optimal structure for the required limit-states, until convergence. The deterministic optimization process is carried out by external software and the reliability assessment is performed through an efficient inverse Most Probable Point (MPP) search algorithm. The MPP is defined as the most probable value of the random variables when reaching the limit-states of the structure $G_i=0$ and represents the nearest point of this function to the mean values of the random variables in a standard and independent space (Choi et al. 2007). This distance is the so-called reliability index β , which is related to the probability of failure of the structure by the following equation when the random variables are normally distributed:

$$P_f = \Phi(-\beta) \quad (2)$$

Therefore, when there are several limit-state functions $G_i=0$, there must be a MPP_i associated to each one. The algorithm used is the Hybrid Mean Value (HMV) by Youn et al. (2003) which finds the MPP_i in the standard and independent space exploring the hyper-sphere with radius β^T (target reliability index of the structure) and center in the mean values (origin of the space), and determining the points where it is tangent to each limit-state function $G_i=0$. Moreover, the HMV is robust since it is suitable for both concave and convex limit-state functions as it combines the Advanced Mean Value (AMV) or the Conjugate Mean Value (CMV) algorithms, both described in Youn et al. (2003). Figure 1 shows a flowchart of the process.

3 Implementation of the methodology

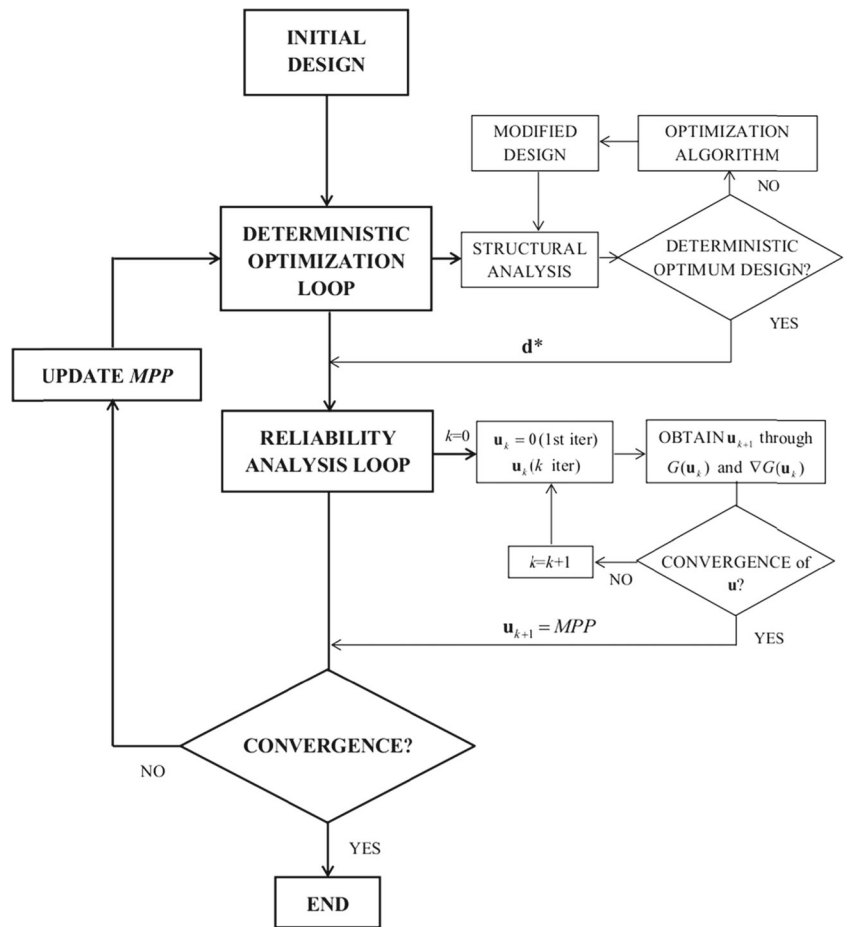
The aim of this work is to develop a framework to solve practical aeronautical RBTO problems embedding optimization software within a RBDO algorithm implemented in an in-house MATLAB (2013) code so as to compute the probabilistic constraints when uncertainty is taken into account in the optimization process. Some parameters that in a deterministic approach would be considered as fixed parameters are now considered as random variables. This methodology excels in being capable of applying such a relevant and helpful discipline as RBTO in large structural models while maintaining the robustness and accuracy of the algorithms employed as well as competitiveness in terms of computational effort. The deterministic optimization software employed is Altair OptiStruct (2013) and was selected because it is widely used in aeronautical companies as Boeing or Airbus, being employed in this research for performing both deterministic optimizations and static analyses. The RBDO algorithm implemented in MATLAB is the SORA, which as discussed in section 2 is a decoupled method that allows exploiting the strengths of the optimization software to perform DTO while adding a reliability analysis not available within it.

In this research two different approaches have been proposed depending on the baseline Finite Element Model (FEM):

- *CASE I:* The baseline FEM is a preliminary structural design. The topology optimization is only performed in a specific domain embedded in the baseline FEM. The objective of this approach is to optimize the layout of selected components within a larger aeronautical structure.
- *CASE II:* The baseline FEM is not a preliminary structural design and the initial model is the complete topology design region. The objective of this approach is to find novel architectures from a prefixed domain.

The design variables d are the relative material densities in all finite elements and the random variables x are the load multiplier factors and the Young's modulus of the material. The strategy followed is to minimize the volume of the design region subject to probabilistic constraints over compliance values. Since the compliance of the structure is associated to a load case, in this work the number of load cases concurs with the number of limit-state functions, so there will be a Most Probable Point (MPP) of failure associated to each one. Below it is presented an explanation of the strategy followed for each case.

Fig. 1 Flowchart of the decoupled RBDO method employed



3.1 CASE I

In this case the compliance of the preliminary design for each load case C_i^U is taken as the reference value for the probabilistic constraints in the upcoming RBTO problem. It is obtained through a previous static analysis of the baseline structure. The goal is to obtain a design as stiff as the preliminary one when uncertainty is included in the problem. Therefore the formulation of the RBTO problem can be expressed mathematically as:

$$\min V(\mathbf{d}_k) \tag{3.a}$$

subject to:

$$P[C_i(\mathbf{d}_k, \mathbf{x}_{i,k}) > C_i^U] \leq P_{f,i} \quad (i = 1, \dots, n) \tag{3.b}$$

where $\mathbf{x}_{i,k}$ is the *MPP* vector with the values of the random variables for the *i*-esime load case in the *k*-esime iteration of the SORA process, *V* is the volume of the design region, C_i is the *i*-esime compliance value obtained in the RBTO process, C_i^U is the compliance upper limit obtained in the static analysis for the *i*-esime load case and *n* is the number of load cases and therefore the number of limit-state functions considered.

3.2 CASE II

The initial design is exactly the prefixed topology design region therefore there is not a proper initial structure. Then a previous DTO process is performed in order to find a preliminary structural scheme. The formulation of this DTO problem consists of minimizing the volume subject to Von Mises stress constraints, and is expressed as:

$$\min V(\mathbf{d}_k) \tag{4.a}$$

subject to:

$$\sigma(\mathbf{d}_k) \leq \sigma_{\max} \tag{4.b}$$

where σ is the Von Mises stress at each element, and σ_{\max} is the maximum admissible Von Mises stress. The DTO is solved using Altair OptiStruct following a SIMP approach.

The compliance of the resulting structural layout C_i^U is taken as the reference value for setting the probabilistic constraints in the upcoming RBTO problem. Now the target is the same as in CASE I, that is, to obtain a design as stiff as the preliminary structural scheme provided by the DTO when uncertainty is taken into account. The mathematical formulation of this RBTO problem is:

$$\min V(\mathbf{d}_k) \tag{5.a}$$

subject to:

$$\sigma(\mathbf{d}_k, \mathbf{x}_{i,k}) \leq \sigma_{\max} \tag{5.b}$$

$$P[C_i(\mathbf{d}_k, \mathbf{x}_{i,k}) > C_i^U] \leq P_{f,i} \quad (i = 1, \dots, n) \tag{5.c}$$

where C_i is the i -esime compliance value of the RBTO and C_i^U is the compliance upper limit obtained from the previous DTO defined in Eq. (4) for the i -esime load case.

These formulations allow obtaining optimal-weight structural architectures while maintaining a required level of stiffness that is defined for each particular problem. The authors believe that these approaches fit better with practical aeronautical problems than the classical minimum compliance with volume fraction constraint. The latter approach needs to impose as a constraint a maximum fraction of the initial volume that is usually chosen by the engineer based on his experience or intuition, while the formers avoid any decision making as these constraints are obtained from a reference design. In contrast to other approaches, both cases require to perform preliminary tasks (a static analysis in CASE I and a DTO in CASE II) so as to set the probabilistic constraints limits C_i^U .

The MATLAB code manages the entire process according to the flowchart of Fig. 2. DTO and the reliability analysis are performed in an iterative process until convergence. For the reliability analysis a target reliability index β^T is considered.

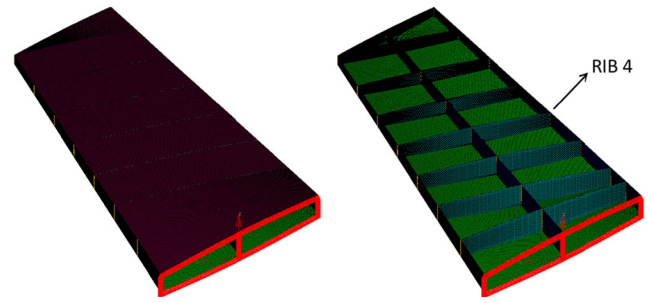


Fig. 3 Three-dimensional view of the aircraft wing structure

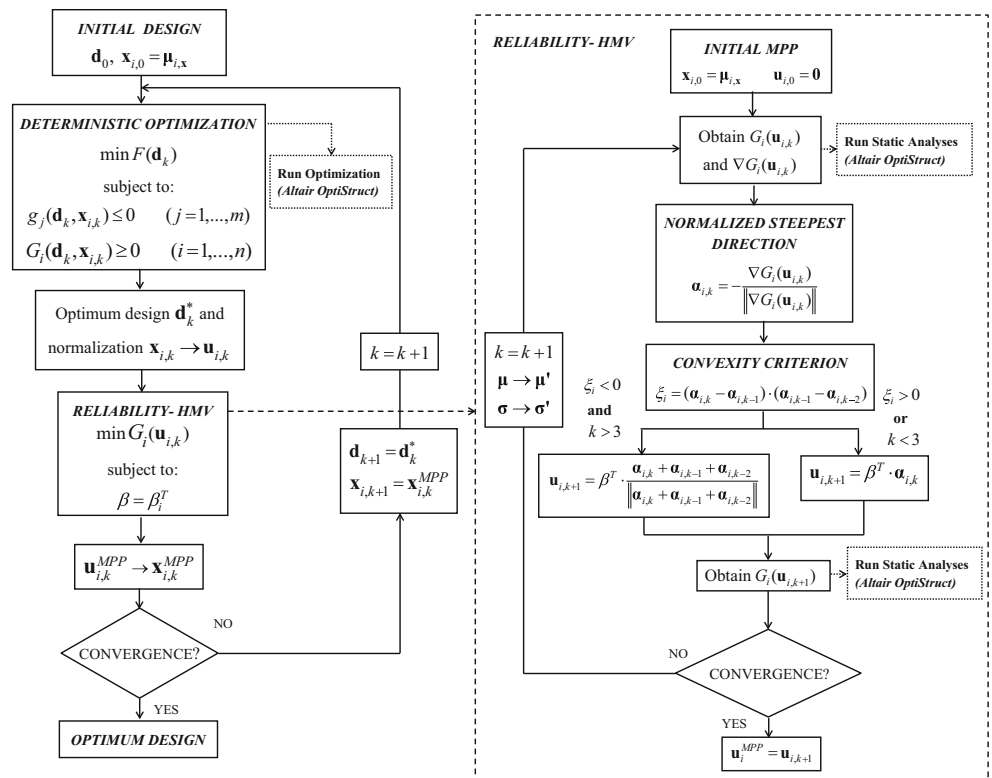
The code starts by the execution of the optimization software so as to reach the initial deterministic solution obtaining the compliance of the optimal structure $C_i(\mathbf{u}_{i,k})$. In this initial optimization process the random variables are set to their mean values. After that, the iterative process of the reliability assessment is started following the steps of the HVM algorithm needed to achieve the MPP of the random variables which will take part in the next optimization cycle.

The first step of the HVM algorithm requires transforming vector \mathbf{x}_i to the standard and independent space \mathbf{u}_i by employing the well-known transformation:

$$\mathbf{u}_{i,k} = \frac{\mathbf{x}_{i,k} - \boldsymbol{\mu}'_{i,x}}{\boldsymbol{\sigma}'_{i,x}} \tag{6}$$

where $\boldsymbol{\mu}'_i$ and $\boldsymbol{\sigma}'_i$ are the mean and standard deviation values that define the equivalent Normal distribution of the random variables x_i , i is the i -esime load case and k is the k -esime

Fig. 2 Flowchart of the SORA method implemented in the MATLAB code using the HVM algorithm for the reliability analysis



iteration of the HMV algorithm (Youn et al. 2003). As the values of vector \mathbf{x}_i initially take their mean values, this corresponds to $\mathbf{u}_{i,0}=\mathbf{0}$. Afterwards, the limit-state functions need to be calculated as stated below:

$$G_i(\mathbf{u}_{i,k}) = 1 - \frac{C_i(\mathbf{u}_{i,k})}{C_i^U} = 0 \tag{7}$$

being $C_i(\mathbf{u}_{i,k})$ the compliance obtained during the previous optimization cycle and C_i^U the limit constraints values. As discussed before, C_i^U is obtained depending on the problem case (CASE I or CASE II). Next, the gradients of the limit-state functions respect to the random variables are obtained through a forward finite difference process expressed by $\nabla G_i(\mathbf{u}_{i,k}) = \frac{G_i(\mathbf{u}_{i,k+h}) - G_i(\mathbf{u}_{i,k})}{h}$, where h is the step size which is set up as a 1 % of the current value of $\mathbf{u}_{i,k}$. This requires several evaluations of the optimal structural compliance after slight perturbations of the random variables. The compliance values are obtained through static analyses of the optimal structural model that are performed in Altair OptiStruct. These gradients are necessary to obtain the normalized steepest descent direction $\alpha_{i,k}$ at the current MPP $\mathbf{u}_{i,k}$, which is defined as follows:

$$\alpha_{i,k} = - \frac{\nabla G_i(\mathbf{u}_{i,k})}{\|\nabla G_i(\mathbf{u}_{i,k})\|} \tag{8}$$

being ∇G_i the aforementioned gradients of the limit-state functions respect to the random variables.

The upcoming $\mathbf{u}_{i,k+1}$ is obtained following the HMV algorithm, being necessary to define a function type criterion to distinguish whether the limit-state function is concave or convex in that particular point. This criterion is expressed by:

$$\xi_i = (\alpha_{i,k} - \alpha_{i,k-1}) \cdot (\alpha_{i,k-1} - \alpha_{i,k-2}) \tag{9}$$

If $\xi_i > 0$, the limit-state function $G_i=0$ is convex, and if $\xi_i \leq 0$ the function is concave. For convex limit-state functions or while $k < 3$, the next point $\mathbf{u}_{i,k+1}$ is obtained as:

$$\mathbf{u}_{i,k+1} = \beta^T \cdot \alpha_{i,k} \tag{10}$$

Otherwise, if the function is concave and $k \geq 3$, the next point $\mathbf{u}_{i,k+1}$ is obtained by combining the steepest descent directions of the three previous iterations with an equal weight, meaning that the algorithm advances in the direction of the diagonal of $\alpha_{i,k}, \alpha_{i,k-1}, \alpha_{i,k-2}$ with a modulus of β^T . This is expressed as:

$$\mathbf{u}_{i,k+1} = \beta^T \cdot \frac{\alpha_{i,k} + \alpha_{i,k-1} + \alpha_{i,k-2}}{\|\alpha_{i,k} + \alpha_{i,k-1} + \alpha_{i,k-2}\|} \tag{11}$$

Once $\mathbf{u}_{i,k+1}$ is obtained, the algorithm returns to (7) to compute a new $G_i(\mathbf{u}_{i,k+1})$. This iterative process reaches convergence when condition (12) is fulfilled:

$$|G_i(\mathbf{u}_{i,k+1}) - G_i(\mathbf{u}_{i,k})| \leq \varepsilon \tag{12}$$

where ε is the maximum convergence criterion value. The flowchart of the HMV algorithm implemented in the MATLAB code to solve the reliability analysis loop is shown in the right side of Fig. 2.

After convergence of HMV algorithm the point $\mathbf{u}_{i,k+1}$ is saved as the MPP \mathbf{u}_i^{MPP} associated to the i -esime limit-state function, and thus the vector of random variables $\mathbf{x}_{i,k+1}$ can be calculated from (6).

The vector $\mathbf{x}_{i,k+1}$ represents the MPP in the original space, and it is used in the upcoming $k+1$ deterministic optimization cycle. The convergence criterion is defined as the difference of the structural volume in two consecutive iterations:

$$|V_{k+1} - V_k| \leq \varepsilon \tag{13}$$

4 A method for coherent comparison between deterministic and reliability-based topology optimization

In the engineering community it is accepted that probabilistic approaches are more realistic than the deterministic ones because the former add the fact that some properties of the design process have not fixed values, so they should be dealt with as random variables. In that regards probabilistic approaches are a better representation of reality.

Comparison between deterministic and probabilistic optima is an important issue that deserves to be studied. In every optimization problem if, after a deterministic optimum is obtained, a RBDO is carried out considering the set of loads and material properties as random variables having as mean values the ones used as fixed parameters in the deterministic approach, the volume of the material obtained in the RBDO will be greater than the obtained in the deterministic. But this comparison is not fair. To check if the RBDO produces heavier or lighter structures a proper comparison must be made. In this research we compare DTO and RBTO.

It is well known that in real problems engineers use in the design the nominal or characteristic load values amplified by a safety coefficient. This coefficient is a way to take into account uncertainties in the expected values of the load. That means that the deterministic design is not fully safe, there is a probability of failure but the designer does not know it. Finding this probability of failure is a way to create a coherent comparison between DTO and RBTO. The approach taken in this research is the following:

1. Assume that any load P_i and the Young's modulus E of the structure are random variables defined by their mean value μ and standard deviation σ .
2. Carry out a DTO problem using as values of P_i and E the following expressions:

$$P_i = \mu_{P,i} + \sigma_{P,i} \cdot \alpha_{P,i} \quad E = \mu_E + \sigma_E \cdot \alpha_E \quad (14)$$

These expressions are only valid when the variables follow a Normal distribution. If the random variables are not normally distributed (uniform, Log-Normal, etc.), their distributions should be transformed to multivariate normal distributions as stated in Nataf (1962) or Rackwitz and Fiessler (1976) before using (14) in order to obtain the statistical moments of the equivalent Normal distribution (μ' , σ').

The output of this step will be a value of the deterministic optimum V^{DTO} .

3. Perform a reliability analysis considering a set of constraints as limit-state functions to find out the probability of failure of the design obtained in step 2 using the random distribution of P_i and E . When any of the random variables is not normally distributed, the Rackwitz and Fiessler transformation must be established in each iteration of the reliability analysis loop so as to obtain the equivalent statistical moments (μ' , σ') for each design point. As a result, a $P_{f,i}^{DTO}$ will be obtained for the i -esime constraint.
4. Carry out a RBTO considering P_i and E as random variables with the former density functions and imposing the same probability of failure $P_{f,i}^{DTO}$ obtained in step 3. As exposed in step 3, (μ' , σ') must be obtained in each iteration of the reliability analysis if any of the random

variables of the problem does not follow a Normal distribution. The output of this formulation will be the volume V^{RBTO} .

With this procedure V^{DTO} and V^{RBTO} can be fairly compared as they are a pair of results having the same probability of failure. Therefore a parameter s_r coined as saving ratio can be defined as:

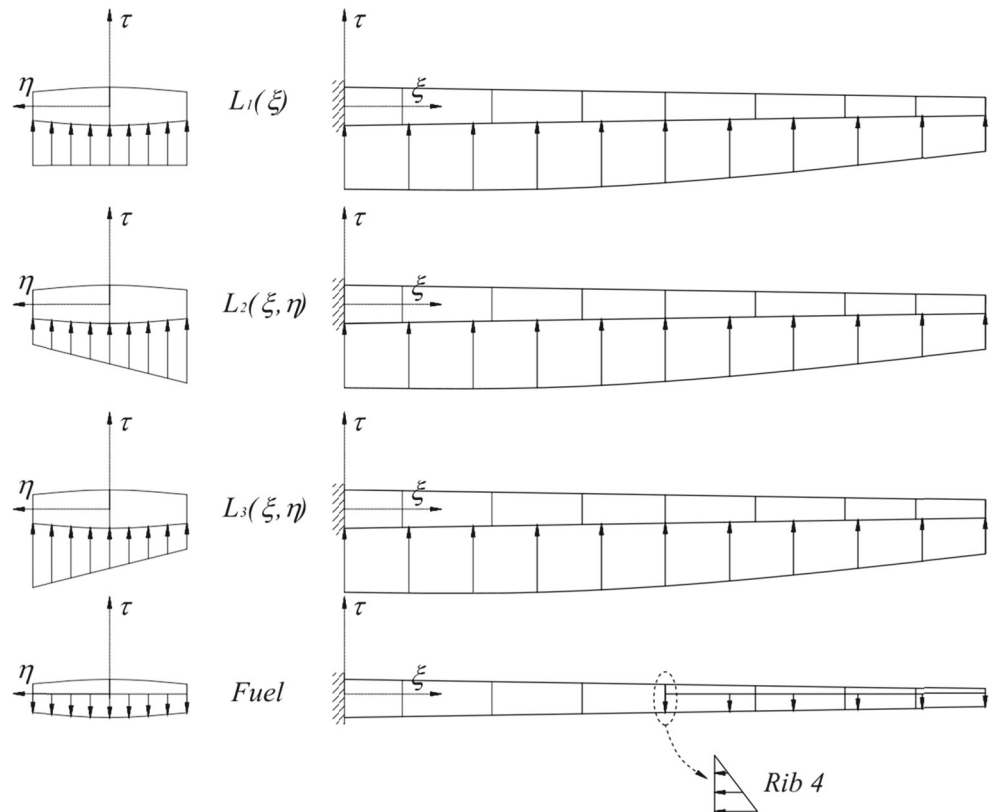
$$s_r = \frac{V^{RBTO}}{V^{DTO}} \quad (15)$$

If $s_r < 1$ that means that the reliability base optimization is more efficient that the deterministic one, as it needs less volume of material to accomplish the same probability of failure for a determined limit-state. In the following application examples this approach has been used to show the performance of the RBTO.

5 Application examples

In order to illustrate the effectiveness of the methodology described in section 3 and to establish a fair comparison between DTO and RBTO as stated in section 4, two large FEMs with around half-million degrees of freedom have been chosen. The first is a 3D shell aircraft wing and the second is a 3D solid aircraft tail-fuselage.

Fig. 4 Applied loads in the aircraft wing structure



5.1 Aircraft wing

The aircraft wing model (Fig. 3) is defined as an assembly of two plates joined by three spars and eight ribs, building a 120816 four-node shell element mesh. The wing root is clamped to the fuselage, and its dimensions are:

- 1219.2 mm of root chord
- 744.22 mm of tip chord
- 152 mm height
- 2463 mm of span
- 26.56° of sweep angle
- 4 mm of ribs and skin thicknesses
- 3 mm of spar thicknesses

The material considered in the ribs is aluminum with a Young’s modulus of $E_r=71000$ MPa, while for the spars and skin is aluminum with Young’s modulus of $E_s=69000$ MPa. Both materials have a density of $\rho=2.7 \cdot 10^{-6}$ kg/mm³.

We consider five different loads expressed in MPa and contained in four load cases. The first load case is constituted by fuel and self-weight loads. Fuel loads are applied only from the wing root to Rib 4 simulating the fuel storage, including both the hydrostatic pressure pushing Rib 4 and a constant pressure of $Q=-0.02$ MPa in gravity direction applied in the bottom skin. Moreover, there are three different lift cases, each constituting one of the remaining load cases. The first is a pure-lift load $L_1(\xi)$ where pressure is applied in the bottom skin following (16):

$$L_1(\xi) = \frac{k_a \cdot \sqrt{2 \cdot S^2 - \xi^2}}{b_{med}} \tag{16}$$

where ξ is the longitudinal local axis of the wing. Moreover, S is the span of the wing and b_{med} is its average transversal dimension, both measured in mm. The lift profile coefficient k_a is obtained through (17):

$$Lift = \frac{\pi \cdot S^2 \cdot k_a}{4} \tag{17}$$

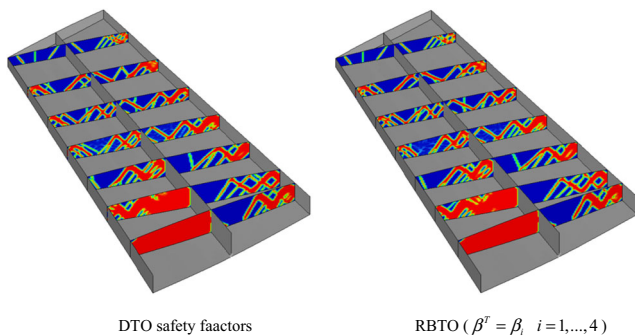


Fig. 5 Comparison between wing structural layout of DTO and RBTO ($\beta^i = \beta_i, i=1, \dots, 4$)

Table 1 Summary of load cases applied in aircraft wing

Load case	Loads multiplier factors				
	Self-weight	Fuel (Q)	Lift 1 ($L_1(\xi)$)	Lift 2 ($L_2(\xi, \eta)$)	Lift 3 ($L_3(\xi, \eta)$)
LC 1	1.0	1.0			
LC 2			1.0		
LC 3				1.0	
LC 4					1.0

being *Lift* the total lift over the wing, which is defined through a critical load case of the aircraft. Based on previous experience, James et. al (2014) used a $2 \cdot g$ maneuver flight load case which corresponds to $Lift=2 \cdot Weight$ and that is employed in this work. The second $L_2(\xi, \eta)$ and third $L_3(\xi, \eta)$ lift-loads are defined as a combination of the pure-lift defined in (16) and a torsional load, simulating that the lift is greater in the frontal part of the wing and lower in the rear part and vice versa. They are modelled as pressure loads and obtained through (18).

$$L_2(\xi, \eta) = 0.85 \cdot \eta + L_1(\xi) \tag{18.a}$$

$$L_3(\xi, \eta) = -0.85 \cdot \eta + L_1(\xi) \tag{18.b}$$

where η is the transversal local axis of the wing. Figure 4 shows an overview of the loads acting in the wing and Table 1 presents a summary of the four load cases applied in this model. The load cases have been defined as equivalent static loads because topology optimization is usually performed in early design stages where the target is to find novel architectures that are later converted to detailed structural components.

The random variables considered in the problem are the loads P by means of the load multiplier factors of each load case ϕ_i and the Young’s modulus of the material E , both following a Normal distribution whose mean and standard deviation values are presented in Table 2.

As exposed in section 4, to perform the DTO we do not employ the mean values of the random variables. Instead we use the design values which are obtained from (14) applying a factor of $\alpha_P = \alpha_E = 1.5$. However, this procedure is general and we could use any value of α .

The design region considered in the wing is the seven inner ribs internal framework. The outer rib is not considered within the design region as the wing must be a closed box. The DTO problem consist of minimizing the volume of the aforementioned

Table 2 Mean and standard deviation values of the random variables

Random variable	Type of distribution	μ	σ
Ribs Young’s modulus (E_r)	Normal	71,000	3550
Load multiplier factor (ϕ_i)	Normal	1.0	0.05

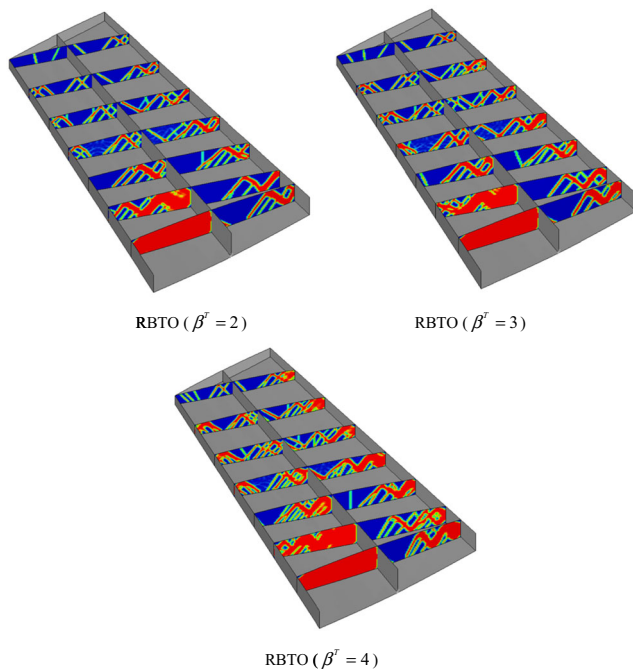


Fig. 6 Wing structural layouts of different RBTO approaches ($\beta^T=2$, $\beta^T=3$ and $\beta^T=4$)

internal framework, which must be as stiff as the one of the preliminary structural design as exposed in section 3 (CASE I). The compliance values obtained from the static analysis of the preliminary design are: $C_1^{STAT}=8.74 \cdot 10^2$ mm/N, $C_2^{STAT}=1.76 \cdot 10^3$ mm/N, $C_3^{STAT}=1.94 \cdot 10^3$ mm/N and $C_4^{STAT}=1.87 \cdot 10^3$ mm/N. The problem is expressed mathematically as:

$$\min V \tag{19.a}$$

subject to:

$$C_i \leq C_i^{STAT} \quad i = 1, \dots, 4 \tag{19.b}$$

where V is the total volume of the design region, i is the considered load case, C_i is the compliance of the design region for each load case and C_i^{STAT} is the upper constraint compliance.

Table 3 Summary results of the comparison DTO vs. RBTO in the aircraft wing

Load case	DTO safety factors	RBTO ($\beta^T=\beta_i=1, \dots, 4$)	s_r
Obj. function (mm^3)	$7.90 \cdot 10^1$	$7.69 \cdot 10^1$	0.97
Initial volume frac. (%)	48.9	47.6	
Value/MPP self weight	1.15	1.16	
Value/MPP fuel loads	1.15	1.02	
Value/MPP lift 1	1.15	1.15	
Value/MPP lift 2	1.15	1.18	
Value/MPP lift 3	1.15	1.16	
Value/MPP young's M.(MPa)	$6.57 \cdot 10^4$	$6.71 \cdot 10^4$	

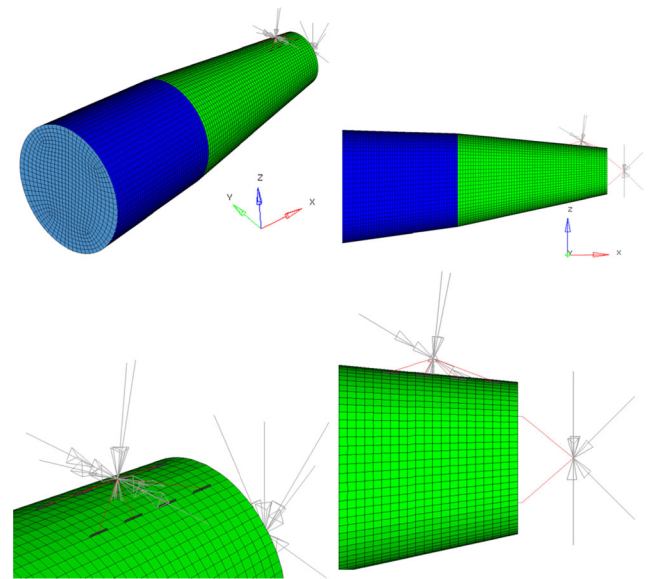


Fig. 7 Side and three-dimensional views of the aircraft tail-fuselage

When the optimum design is reached, a reliability analysis using the First Order Reliability Method (FORM) is performed in order to obtain the probability of failure of the structure for each limit-state function using the random distributions of P and E . The limit-state functions for all load cases are defined as (7). As a result, a set of probability of failures is obtained, which corresponds to $\beta_1=3.60$, $\beta_2=3.39$, $\beta_3=4.01$ and $\beta_4=3.47$.

Afterwards, the RBTO problem is performed as explained in section 3 (CASE I). The target of this problem is to obtain a design whose internal framework is as stiff as the one of the preliminary design when uncertainty is contemplated in both loads P and Young's modulus E . We impose the same probability of failure obtained in the previous reliability analysis so as to make a right comparison between DTO and RBTO approaches. The mathematical formulation of the latter is:

$$\min V \tag{20.a}$$

subject to:

$$P[C_i > C_i^{STAT}] \leq P_{f,i} \quad i = 1, \dots, 4 \tag{20.b}$$

Table 4 Summary results of the set of RBTO in the aircraft wing

Load case	RBTO ($\beta^T=2$)	RBTO ($\beta^T=3$)	RBTO ($\beta^T=4$)
Obj. function (mm^3)	$6.11 \cdot 10^1$	$7.16 \cdot 10^1$	$8.64 \cdot 10^1$
Initial volume frac. (%)	37.8	44.3	53.4
MPP self weight	1.09	1.13	1.17
MPP fuel loads	1.01	1.02	1.05
MPP lift 1	1.09	1.13	1.19
MPP lift 2	1.09	1.14	1.18
MPP lift 3	1.09	1.14	1.18
MPP young's M.(MPa)	$6.88 \cdot 10^4$	$6.66 \cdot 10^4$	$6.8 \cdot 10^4$

Fig. 8 Comparison between DTO with safety factors and RBTO ($\beta^T=3.83$) layouts

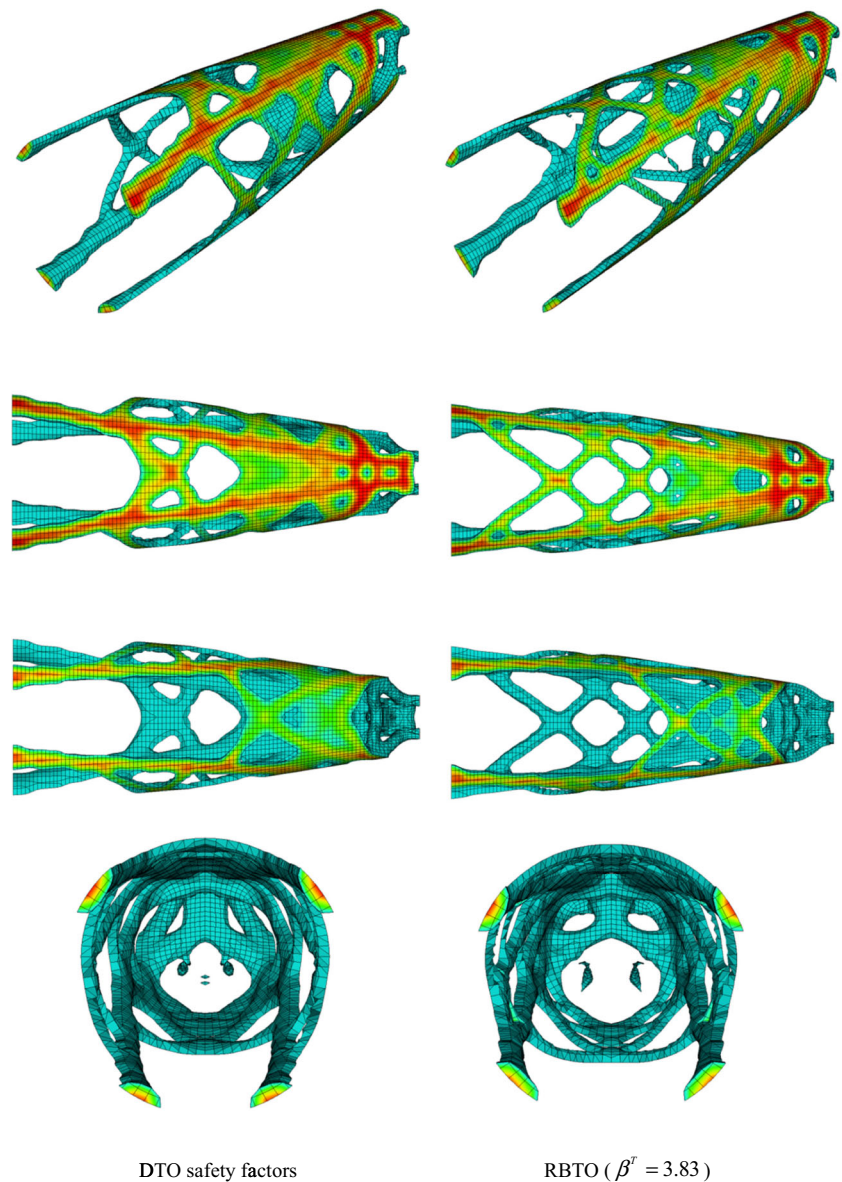


Figure 5 shows the results obtained from both DTO and RBTO, hiding the top skin of the wing so as to provide a clear view of the wing ribs (design region). Table 3 shows a clear comparison between both approaches, obtaining a saving ratio

of $s_r=0.97$ as the RBTO draws a 3 % lower volume than DTO for the same probability of failure.

In addition we perform a set of RBTO cases for different safety targets of

Table 5 Loads applied to the aircraft tail-fuselage FEM

Load case	Loads in vertical tail plane (N and $N \cdot mm$)						Loads in rear fuselage (N)		
	F_x	F_y	F_z	M_x	M_y	M_z	F_x	F_y	F_z
LC 1	0	$-1 \cdot 10^5$	0	$2.5 \cdot 10^8$	0	$1.5 \cdot 10^8$	0	$-8 \cdot 10^3$	$-12 \cdot 10^3$
LC 2	0	$1 \cdot 10^5$	0	$-2.5 \cdot 10^8$	0	$-1.5 \cdot 10^8$	0	$8 \cdot 10^3$	$12 \cdot 10^3$
LC 3	$-1 \cdot 10^4$	0	$-1 \cdot 10^5$	0	$4 \cdot 10^8$	0	0	0	$-28 \cdot 10^3$
LC 4	$1 \cdot 10^4$	0	$1 \cdot 10^5$	0	$-4 \cdot 10^8$	0	0	0	$28 \cdot 10^3$
LC 5	$2 \cdot 10^4$	0	$1 \cdot 10^5$	0	$-5 \cdot 10^8$	0	$-8 \cdot 10^3$	0	$8 \cdot 10^3$
LC 6	$-2 \cdot 10^4$	0	$-1 \cdot 10^5$	0	$5 \cdot 10^8$	0	$-8 \cdot 10^3$	0	$-8 \cdot 10^3$

$\beta^T=2$, $\beta^T=3$ and $\beta^T=4$, which corresponds to probabilities of failure of $P_f=2.27 \cdot 10^{-2}$, $P_f=1.35 \cdot 10^{-3}$ and $P_f=3.17 \cdot 10^{-5}$ respectively. As expected, requesting a higher reliability brings an increase in the member size of the structure, but also to some changes in the structural layout, being the latter consequence difficult to predict using only engineering judgment. Figure 6 and Table 4 show the results obtained.

5.2 Aircraft tail-fuselage

The three-dimensional tail-fuselage model is composed by two non-concentric tail cones connected, with greater radii of 2.1 and 1.75 m and lower radii of 1.75 and 0.45 m, respectively. Both parts are merged in the junction and the whole model length is 10 m. All degrees of freedom are constrained in the front part of the fuselage, and two set of loads are applied in the rear part: those transmitted by the vertical tail plane (VTP) and horizontal tail plane (HTP) to the fuselage and those corresponding to the rear fuselage tail cone. The model is discretized by 68136 eight-node solid elements which represent the design region, 7824 four-node shell elements that simulate the external skin of the fuselage, and 18 rigid elements that simulate the load transmission from the VTP, HTP and tail cone to the fuselage. A three-dimensional and a side view of the FEM are shown in Fig. 7, as well as a zoom of the rear part for a clear view of the load transmission to the fuselage.

The material of the structural model is aluminum, with a Young’s modulus of $E=74000$ MPa. The tail fuselage of an aircraft is a region exposed to many different loads as it receives the loads acting in both the VTP and HTP. Therefore, a set of six load cases have been chosen as a representative sample of all load cases acting in a commercial aircraft tail fuselage model. The load cases considered in this example are symmetric in pairs respect to the x - z plane of the aircraft, and are represented in Table 5.

Uncertainty is considered in the applied loads and material properties, becoming the random variables of the problem, and whose mean and standard deviation values are presented in Table 6. The load values for each load case are multiplied by a factor ϕ_i , which is the true random variable. The Young’s module E follows a Log-Normal distribution and the load multiplier factors ϕ_i follow a Normal distribution.

As explained in section 3 (CASE II), a preliminary design is obtained performing a DTO process because the baseline model is not a proper structure, being the whole 3D domain

Table 6 Mean and standard deviation values of the random variables

Random variable	Type of distribution	μ	σ
Young’s modulus (E)	Log-normal	74,000	3700
Load multiplier factor (ϕ_i)	Normal	1.0	0.1

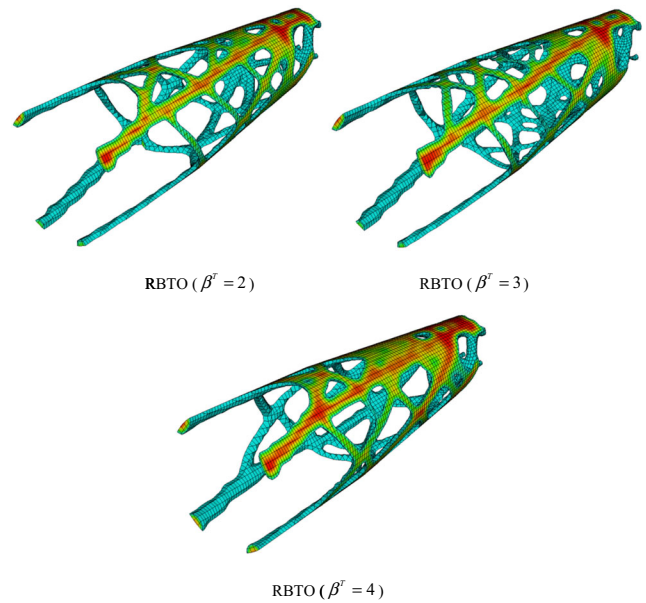


Fig. 9 Three-dimensional view of different RBTO ($\beta^T=2$, $\beta^T=3$ and $\beta^T=4$) layouts

exactly the design region. This preliminary design is employed to obtain the compliance needed to set the stiffness constraints of both DTO and RBTO approaches so as to compare them. The loads and material properties employed in this preliminary DTO are the mean values of the random variables exposed in Table 6, so this approach will be named as DTO-m from now on. This DTO-m problem is formulated mathematically as minimizing the volume of the tail-fuselage region subject to Von Mises stress constraints:

$$\min V \tag{21.a}$$

subject to:

$$\sigma \leq 300 \text{MPa} \tag{21.b}$$

where V is the total volume of the tail fuselage and σ is the Von Mises stress in each element. Once solved the compliance of the

Table 7 Summary results of the comparison DTO vs. RBTO in the aircraft tail fuselage

Load case	DTO safety factors	RBTO ($\beta^T=3.83$)	s_r
Objective function (mm^3)	$4.93 \cdot 10^9$	$4.81 \cdot 10^9$	0.97
Initial volume frac. (%)	5.81	5.67	
Value/MPP load case 1	1.15	1.19	
Value/MPP load case 2	1.15	1.19	
Value/MPP load case 3	1.15	1.12	
Value/MPP load case 4	1.15	1.12	
Value/MPP load case 5	1.15	1.15	
Value/MPP load case 6	1.15	1.15	
Value/MPP young’s M. (MPa)	$6.83 \cdot 10^4$	$7.15 \cdot 10^4$	

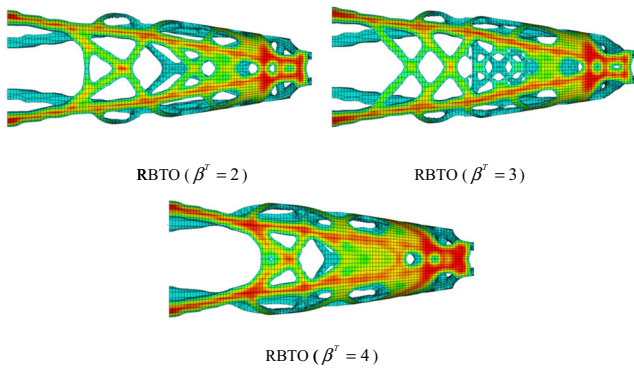


Fig. 10 Top view of different RBTO ($\beta^T=2, \beta^T=3$ and $\beta^T=4$) layouts

optimal structure is obtained for all load cases. In fuselage topology optimization problems it is usual to obtain the information about the weighted compliance of the structure (Niemann et al. 2013) instead of the single compliances for each load case, because as discussed before the number of load cases may be elevated and it may be troublesome to handle. The weighted compliance is defined as the weighted sum of the single compliances for all load cases, and is expressed as follows:

$$WC = \sum_{i=1}^n w_i \cdot C_i \quad (i = 1, \dots, n) \quad (22)$$

where w_i are the weighting factors considered for the i -esimo load case. In this particular example all load cases are equally pondered.

Therefore, the only limit-state function in this problem is associated to the weighted compliance of the tail fuselage, and is expressed as:

$$G = 1 - \frac{WC}{WC^{DTO}} = 0 \quad (23)$$

where WC is the weighted compliance obtained in the upcoming RBTO analyses, WC^{DTO} is the weighted compliance of the preliminary DTO-m design and $G=0$ is the limit-state function. The weighted compliance obtained from the DTO-m is: $WC^{DTO}=4.56 \cdot 10^7$ mm/N.

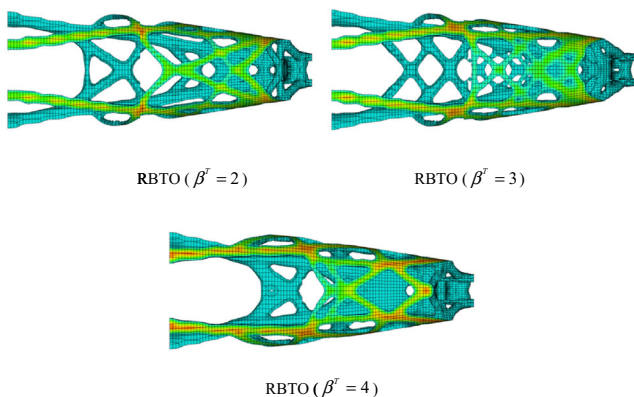


Fig. 11 Bottom view of different RBTO ($\beta^T=2, \beta^T=3$ and $\beta^T=4$) layouts

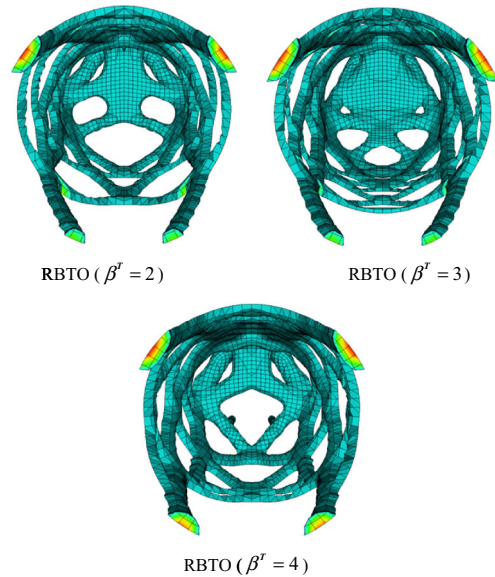


Fig. 12 Frontal view of different RBTO ($\beta^T=2, \beta^T=3$ and $\beta^T=4$) layouts

Next we perform the comparison between the DTO and RBTO approaches. In the DTO the design values of the loads and material properties are obtained from (14) applying a factor of $\alpha_P=\alpha_E=1.5$, although the procedure is general for any value of α , as stated in section 4. Before using (14), in this example the random distribution of the Young's module E has to be converted from a Log-Normal to an equivalent Normal using the Rackwitz and Fiessler (1976) transformation. Once the DTO is completed, the probability of failure of the structure for the limit-state function defined in (23) is computed using the random distributions of P and E . Therefore a reliability analysis using the First Order Reliability Method (FORM) is performed and a reliability index of $\beta=3.83$ is obtained, which corresponds to a probability of failure of $P_f=6.41 \cdot 10^{-5}$ that will then be imposed in the RBTO.

Afterwards the RBTO problem imposing $\beta^T=3.83$ is performed applying the methodology explained in section 3 (CASE II). The target of the RBTO is to obtain a design as stiff as the structural scheme provided by the preliminary

Table 8 Summary results of the set of RBTO in the aircraft tail fuselage

Load case	RBTO ($\beta^T=2$)	RBTO ($\beta^T=3$)	RBTO ($\beta^T=4$)
Objective function (mm^3)	$3.94 \cdot 10^9$	$4.33 \cdot 10^9$	$4.90 \cdot 10^9$
Initial volume frac. (%)	4.64	5.10	5.77
MPP load case 1	1.09	1.14	1.20
MPP load case 2	1.09	1.14	1.20
MPP load case 3	1.07	1.10	1.12
MPP load case 4	1.07	1.10	1.12
MPP load case 5	1.08	1.12	1.15
MPP load case 6	1.08	1.12	1.15
MPP young's M. (MPa)	$7.25 \cdot 10^4$	$7.21 \cdot 10^4$	$7.16 \cdot 10^4$

Table 9 Summary of the computational effort counted in iterations

Example	Loop	DTO	RBTO ($\beta^T=2$)	RBTO ($\beta^T=3$)	RBTO ($\beta^T=4$)
Aircraft wing	Optimization	49 iter.	143 iter.	236 iter.	150 iter.
	Reliability	–	168 iter.	336 iter.	168 iter.
Aircraft fuselage	Optimization	81 iter.	241 iter.	416 iter.	363 iter.
	Reliability	-	48 iter.	96 iter.	72 iter.

DTO-m when uncertainty is taken into account. The formulation of this RBTO problem is:

$$\min V \tag{24.a}$$

subject to:

$$\sigma \leq 300MPa \tag{24.b}$$

$$P[WC > WC^{DTO}] \leq P_f \tag{24.c}$$

The results obtained from the comparison between DTO and RBTO are shown in Fig. 8, hiding the skin of the fuselage and displaying only the design region formed by the solid elements in order to show clearly the structural layouts.

Table 7 shows a clear comparison between both approaches, obtaining a saving ratio of $s_r=0.97$ as the RBTO draws a structural scheme of a 3 % lower volume than the obtained from the DTO, having both the same probability of failure against a determined limit state.

Moreover, a set of additional RBTO cases have been performed for target reliability indexes of $\beta^T=2$, $\beta^T=3$ and $\beta^T=4$ corresponding to probabilities of failure of $P_f=2.27 \cdot 10^{-2}$, $P_f=1.35 \cdot 10^{-3}$ and $P_f=3.17 \cdot 10^{-5}$, respectively. The results obtained for these RBTO approaches are shown in Figs. 9, 10, 11 and 12.

In this example it can be observed that requesting a higher reliability leads to a substantial change in the structural layout, being a worthy remarkable aspect that may influence the next phases of the aircraft design process. Besides, this change in the layout is associated to a significant volume increase because as expected, requiring a higher reliability index takes to heavier designs. Table 8 shows a summary of the results obtained in the set of RBTO analyses.

6 Computational facilities

The examples developed have been solved in a high performance cluster (HPC) with 768 computing cores, a theoretical

peak performance of 5.1 TFLOP’s and a physical memory of 1.8 TB. Table 9 shows a summary with the computational effort in terms of iterations, while Table 10 shows the computational time in minutes for all examples. In addition the computational time to run a single static analysis to obtain the compliance of the structure is about 100 seconds in the wing example and around 120 seconds in the tail-fuselage example. All the cases have been run employing 4 cores of the HPC and assigning a physical memory of 8 GB to each.

In terms of computational time, the aircraft wing took a maximum time of about 15 hours for $\beta^T=3$, while the three-dimensional tail aircraft fuselage took a maximum time of approximately 42 hours for $\beta^T=3$ and $\beta^T=4$. In the rest of cases the range of time is about 8 hours for the aircraft wing and about 25 hours for the aircraft tail fuselage. It is noticeable that performing a RBTO analysis for such complex structural models takes an average of approximately ten to twenty times than solving the DTO in the same example.

7 Conclusions

This paper has proposed a methodology that allows performing large topology optimization problems while taking into account the uncertainty presented in both loads and material properties. This methodology has proven to be robust and efficient as it worked for different 3D structural models and the computational effort spent was acceptable regarding the time that commercial software needs to perform the classical deterministic topology optimization. Furthermore, the Sequential Optimization and Reliability Assessment algorithm has proven to be successfully implementable with commercial software that performs deterministic optimization due to its uncoupled formulation and the auspicious results obtained. To summarize, this research demonstrated that reliability-based topology optimization can be successfully applied to industry-like aircraft structural models as a further step to classical topology optimization.

Table 10 Summary of computational time

Example	DTO	RBTO ($\beta^T=2$)	RBTO ($\beta^T=3$)	RBTO ($\beta^T=4$)
Aircraft wing	59 minutes	513 minutes	989 minutes	518 minutes
Aircraft fuselage	144 minutes	1692 minutes	2532 minutes	2547 minutes

Besides, a comparison between Reliability-Base Topology Optimization and Deterministic Topology Optimization has been made, concluding that the former is a more efficient tool to implement in preliminary design phase as it leads to lighter structural architectures than the latter considering the same probability of failure. Regarding this, RBTO may achieve structures with a higher safety level if the volume is set to be the same as the obtained in the deterministic approach.

In the first example it can be seen that the differences between different safety targets are mainly focused in the appearance of new members when establishing a higher level of uncertainty, as well as the fattening of the members obtained in the deterministic optimization. This concludes that when requiring a higher safety factor in the reliability-based optimization, the amount of material needed to accomplish the constraints increases.

Moreover, it is noticeable that in the second example the structural schemes obtained through deterministic and reliability-based topology optimization are different depending on the level of uncertainty considered, which lead to substantially different novel architectures. This gives an idea of how important is to define the safety level required in the preliminary stages of aircraft design so as to continue with the design process from the best initial architecture.

Acknowledgments The research leading to these results is part of the research project DPI2013-41893-R received from the Spanish Ministry of Economy. Further funding has been received from the Galician Government (including FEDER funding) with reference GRC2013-056 and from the program FPU (University teacher training program) from the Spanish Ministry of Education, Culture and Sports.

References

- Altair Optistruct User Manual (2013) Version 12, Altair Engineering Inc
- Aoues Y, Chateaufort A (2010) Benchmark study of numerical methods for reliability-based design optimization. *Struct Multidiscip Optim* 41(2):277–294. doi:10.1007/s00158-009-0412-2
- Buchanan S (2007) Development of a wingbox rib for a passenger jet aircraft using design optimization and constrained to traditional design and manufacture requirements. Altair Engineering CAE Technology Conference, Michigan
- Choi SK, Grandhi RV, Canfield RA (2007) Reliability-based structural design. Springer, London
- Du X, Chen W (2004) Sequential optimization and reliability assessment method for efficient probabilistic design. *J Mech Des Trans ASME* 126(2):225–233. doi:10.1115/1.1666890
- Dunning P, Kim A, Mullineux G (2011) Introducing loading uncertainty in topology optimization. *AIAA J* 49(4):760–768. doi:10.2514/1.J050670
- Enevoldsen I, Sørensen JD (1994) Reliability-based optimization in structural engineering. *Struct Saf* 15(3):169–196. doi:10.1016/0167-4730(94)90039-6
- Grihon S, Krog L, Tucker A, Hertel K (2004) A380 weight savings using numerical structural optimization. 20th AAAF colloquium on material for aerospace applications, Paris, France; 763–766
- Hernandez S, Diaz J, Baldomir A, Cid M, López C (2013) Comparison of reliability based structural optimization methodologies in the design of aircraft structures. Safety, reliability, risk and life-cycle performance of structures and infrastructures—Proceedings of the 11th International Conference on Structural Safety and Reliability, ICCOSSAR 2013. New York, NY, 4943–4949
- James KA, Kennedy GJ, Martins JRRA (2014) Concurrent aerostructural topology optimization of a wing box. *Comput Struct* 134:1–17. doi:10.1016/j.compstruc.2013.12.007
- Jung HS, Cho S (2004) Reliability-based topology optimization of geometrically nonlinear structures with loading and material uncertainties. *Finite Elem Anal Des* 43(3):311–331. doi:10.1016/j.finell.2004.06.002
- Kang Z, Luo Y (2009) Non-probabilistic reliability-based topology optimization of geometrically nonlinear structures using convex models. *Comput Methods Appl Mech Eng* 198(41–44):3228–3238. doi:10.1016/j.cma.2009.06.001
- Kang JN, Kim CI, Wang SM (2004) Reliability-based topology optimization for electromagnetic systems. *COMPEL - Int J Comput Math Electric Electron Eng* 23(3):715–723. doi:10.1108/03321640410540647
- Karadeniz H, Togan V, Vrouwenvelder T (2009) An integrated reliability-based design optimization of offshore towers. *Reliab Eng Syst Saf* 94:1510–1516. doi:10.1016/j.res.2009.02.008
- Kaushik S (2007) Reliability-based multiobjective optimization for automotive crashworthiness and occupant safety. *Struct Multidiscip Optim* 33(3):255–268. doi:10.1007/s00158-006-0050-x
- Kharmanda G, Olhoff N, Mohamed A, Lemaire M (2004) Reliability based topology optimization. *Struct Multidiscip Optim* 26(5):295–307. doi:10.1007/s00158-003-0322-7
- Kim C, Wang S, Bae K-R, Moon H, Choi KK (2006) Reliability based topology optimization with uncertainties. *J Mech Sci Technol* 20(4):494–504. doi:10.1007/BF02916480
- Kim C, Wang S, Hwang I, Lee J. (2007) Application of reliability based topology optimization for microelectromechanical systems. *AIAA J* 45(12) 2926–2934. doi: 10.2514/1.28508
- Krog L, Tucker A (2002) Application of topology, sizing and shape optimization methods to optimal design of aircraft components. Altair Engineering Conference
- Krog L, Tucker A, Kemp M, Boyd R (2004) Topology optimization of aircraft wing box ribs. 10th AIAA/ ISSMO multidisciplinary analysis and optimization conference, code 65014, volume 3, Albany, New York, 2020–2030
- MATLAB R2013a (2013) Documentation
- Maute K, Allen M (2004) Conceptual design of aeroelastic structures by topology optimization. *Struct Multidiscip Optim* 27(1–2):27–42. doi:10.1007/s00158-003-0362-z
- Maute K, Frangopol DM (2003) Reliability-based design of MEMS mechanisms by topology optimization. *Comput Struct* 81(8–11):813–824. doi:10.1016/S0045-7949(03)00008-7
- Maute K, Reich GW (2006) Integrated multidisciplinary topology optimization approach to adaptive wing design. *AIAA J Aircraft* 43(1):253–263. doi:10.2514/1.12802
- Nataf A (1962) Détermination des distributions de probabilités dont les marges sont donnés. *C R Acad Sci* 225:42–43
- Nguyen TH, Song J, Paulino GH (2011) Single-loop system reliability based topology optimization considering statistical dependence between limit states. *Struct Multidiscip Optim* 44(5):593–611. doi:10.1007/s00158-011-0669-0
- Niemann S, Kolesnikov B, Lohse-Busch H, Hühne C, Querin OM, Toropov VV, Liu D (2013) The use of topology optimization in the conceptual design of next generation lattice composite aircraft fuselage structures. *Aeronaut J* 117(1197):1139–1154
- Rackwitz R, Fiessler B (1976) Note on discrete safety checking when using non-normal stochastic models for basic variables. load project working session. MIT, Cambridge

- Santos IR, Rocha de FA (2013) Topology optimization of multiple load case structures. IV International Symposium on Solid Mechanics—MecSol 2013. Porto Alegre, Rio Grande do Sul, Brazil
- Silva M, Tortorelli DA, Norato J, Ha C, Bae HR (2010) Component and system reliability-based topology optimization using a single loop method. *Struct Multidiscip Optim* 41(1):87–106. doi:10.1007/s00158-009-0401-5
- Stanford B, Dunning P (2014) Optimal topology of aircraft rib and spar structures under aeroelastic loads. 10th AIAA Multidisciplinary Design and Optimization Specialist Conference, Code 102896. AIAA, National Harbor
- Stanford B, Ifju P (2009) Aeroelastic topology optimization of membrane structures for micro air vehicles. *Struct Multidiscip Optim* 38(3): 301–316. doi:10.1007/s0158-008-0292-x
- Stanford B, Beran P, Kobayashi MH (2012) Aeroelastic optimization of flapping wing venation: a cellular division approach. *AIAA J* 50(4): 938–951
- Tu J, Choi KK, Park YH (1999) A new study on reliability-based design optimization. *J Mech Des Trans ASME* 121(4):557–564. doi:10.1115/1.2829449
- Wang Q, Lu Z, Zhou C (2011) New topology optimization method for wing leading-edge ribs. *AIAA J Aircraft* 48(5):1741–1748. doi:10.2514/1.C031362
- Youn BD, Choi KK, Park YH (2003) Hybrid analysis method for reliability-based design optimization. *J Mech Des Trans ASME* 125(2):221–232. doi:10.1115/1.1561042
- Youn BD, Choi KK, Yang RJ, Gu L (2004) Reliability-based design optimization for crashworthiness of vehicle side impact. *Struct Multidiscip Optim* 26(3–4):272–283. doi:10.1007/s00158-003-0345-0
- Zou T, Mahadevan S (2005) Multi-objective RBDO for automotive door quality design. SAE Technical Paper, Paper 2005-01-0346, Detroit, MI. doi: 10.4271/2005-01-0346